

Brain Hematoma Segmentation Using Active Learning and an Active Contour Model

Heming Yao^{1(⊠)}, Craig Williamson², Jonathan Gryak¹, and Kayvan Najarian^{1,3,4}

- Department of Computational Medicine and Bioinformatics, University of Michigan, Ann Arbor, MI, USA
- ² Department of Neurosurgery, University of Michigan, Ann Arbor, MI, USA
 ³ Michigan Center for Integrative Research in Critical Care, University of Michigan, Ann Arbor, MI, USA
- ⁴ Department of Emergency Medicine, University of Michigan, Ann Arbor, MI, USA {hemingy,craigaw,gryakj,kayvan}@med.umich.edu

Abstract. Traumatic brain injury (TBI) is a massive public health problem worldwide. Accurate and fast automatic brain hematoma segmentation is important for TBI diagnosis, treatment and outcome prediction. In this study, we developed a fully automated system to detect and segment hematoma regions in head Computed Tomography (CT) images of patients with acute TBI. We first over-segmented brain images into superpixels and then extracted statistical and textural features to capture characteristics of superpixels. To overcome the shortage of annotated data, an uncertainty-based active learning strategy was designed to adaptively and iteratively select the most informative unlabeled data to be annotated for training a Support Vector Machine classifier (SVM). Finally, the coarse segmentation from the SVM classifier was incorporated into an active contour model to improve the accuracy of the segmentation. From our experiments, the proposed active learning strategy can achieve a comparable result with 5 times fewer labeled data compared with regular machine learning. Our proposed automatic hematoma segmentation system achieved an average Dice coefficient of 0.60 on our dataset, where patients are from multiple health centers and at multiple levels of injury. Our results show that the proposed method can effectively overcome the challenge of limited and highly varied dataset.

 $\begin{tabular}{ll} \textbf{Keywords:} & \textbf{Medical image segmentation} \cdot \textbf{Medical image processing} \cdot \\ \textbf{Traumatic brain injury} \cdot \textbf{Active learning} \cdot \textbf{Active contour model} \\ \end{tabular}$

1 Introduction

Traumatic brain injury (TBI) is a major cause of death and disability worldwide, especially in children and young adults. Accurate and fast detection and diagnosis of brain damage in the early stage of injury is important for prompt and

[©] Springer Nature Switzerland AG 2019

I. Rojas et al. (Eds.): IWBBIO 2019, LNBI 11466, pp. 385-396, 2019.

proper management of TBI patients [1]. To detect the presence and extent of brain hematoma, Computed tomography (CT) is the imaging modality of choice during the first 48 h after injury [1] due to its speed, low-cost, and availability. Previous studies have shown that brain hematoma detection and volume calculation are important for TBI diagnosis [1], mortality and morbidity prediction [2, 3], and surgical management [4].

To facilitate TBI patient management, an automatic hematoma segmentation system can provide accurate and quantitative evaluations of brain hematoma. It can decrease medical costs and provide guidance for proper medical treatment [4]. Many segmentation methods have been proposed. A semi-automated method based on a region growing algorithm was proposed for brain hematoma [5] that requires seed points fixed by the user. A level set algorithm was developed [6] where candidate hematoma voxels were identified by an adaptive threshold. An algorithm combining Gaussian Mixture Model (GMM) and Expectation Maximization was proposed to find hematoma component [7]. Most of the previous studies rely on either manual initialization or the distribution of intensity values in brain tissues to segment hematoma regions. However, hematoma intensity varies across imaging protocols and patient conditions, and other anatomical structures such as straight sinus exhibit a similar intensity. Moreover, these techniques ignore textural differences between brain tissues and structures.

In this study, to better segment hematoma, we proposed a fully-automatic hematoma segmentation framework that extracts texture features and integrates a supervised model with an active contour model. One challenge here is although there are plenty of medical images available, annotating these images is very time-consuming. To overcome the shortage of labeled images, an active learning strategy is presented. It started with training an initial support vector machine (SVM) model using one annotated image and then queried the most informative superpixels whose labels may lead to the greatest improvement to the model. After active learning, the superpixel-based classification resulted in a coarse hematoma segmentation. The coarse segmentation was incorporated into an active contour model to generate the final fine segmentation.

Our contributions here are two-fold. First, we proposed an active learning algorithm for image segmentation. Our experiments show that the active learning strategy can effectively select the most informative samples whose labels result in a significantly higher performance improvement compared with random selection. From our results, active learning can help overcome the shortage of annotated data, which is a common problem in medicine. Secondly, we proposed a hematoma segmentation framework and achieved a mean Dice coefficient of 0.60 on a challenging dataset. The dataset consists of CT scans from patients with various health conditions and using different imaging protocol, where hematoma regions are of various shapes, types and occur at different locations.

2 Methodology

As shown in Fig. 1, we first adjusted contrast within the CT images and performed skull removal to extract the soft tissues for further analysis. The brain

regions were then over-segmented into superpixels. For each superpixel s_i , statistical and textural features were extracted to generate a feature vector \mathbf{v}_i . The label of each superpixel is denoted by y_i , with $y_i = 1$ when s_i belongs to a hematoma region (i.e. the majority of pixels in s_i belong to a hematoma region) and $y_i = 0$ otherwise. An SVM classifier was trained to predict superpixel class and generate a coarse segmentation map. Finally, the coarse segmentation was used as a segmentation prior for an active contour model to refine the segmentation boundary.

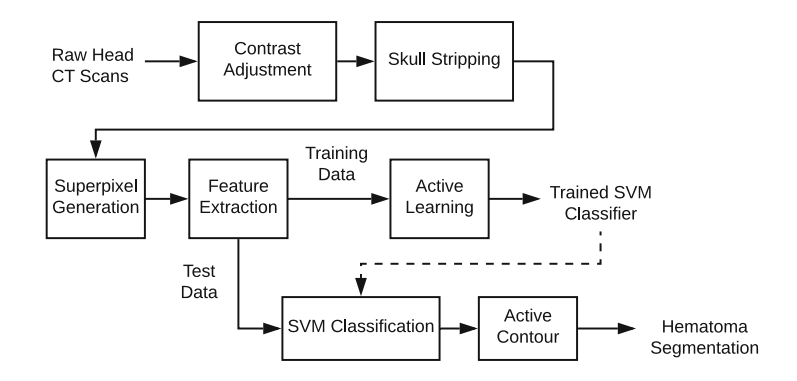


Fig. 1. A diagram of the proposed framework

2.1 Pre-processing

Let us define an image of size $H \times W$ as $I : \Omega \to \mathbb{R}$, where $\Omega = \{1, 2, ..., H\} \times \{1, 2, ..., W\}$. In the first pre-processing step, a linear transformation

$$I_{HU} = I_{raw} \times slope + intercept \tag{1}$$

was performed to convert the gray values stored in Digital Imaging and Communication in Medicine (DICOM) format to Hounsfield units (HU), where I_{raw} is the image with gray values stored in DICOM format, and I_{HU} is the transformed image in HU. slope and intercept are parameters retrieved from the DICOM header file.

Next, contrast adjustment was performed by extracting and scaling the predefined range of HU into 8-bit grayscale, as shown in (2).

$$I_{adj}(\mathbf{x}) = \begin{cases} 0 & I_{HU}(\mathbf{x}) < wc - \frac{ww}{2} \\ (I_{HU}(\mathbf{x}) - (wc - \frac{ww}{2})) \times \frac{255}{ww} & wc - \frac{ww}{2} \le I_{HU}(\mathbf{x}) \le wc + \frac{ww}{2} \\ 255 & I_{HU}(\mathbf{x}) > wc + \frac{ww}{2} \end{cases}$$
(2)

where $I_{adj}(x)$ is the intensity after contrast adjustment at location $x \in \Omega$, and ww and wc are the window width and the window center obtained from the

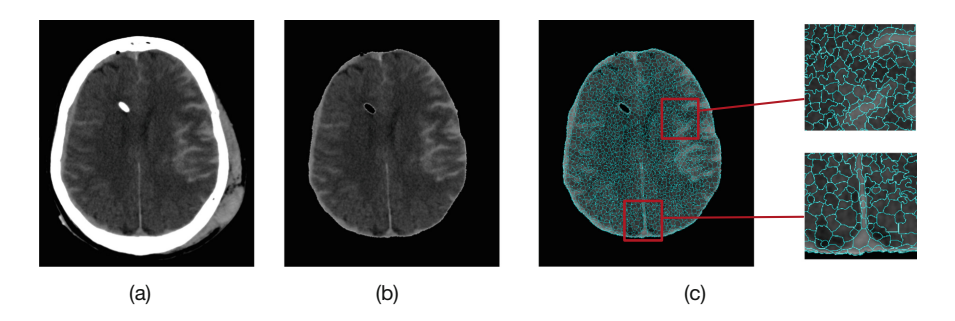


Fig. 2. An illustration of the proposed data preparation (Color figure online). (a) The image after the contrast adjustment. (b) The image after the skull stripping. (c) Superpixel generation.

DICOM header file, respectively. To highlight the appearance and structure of soft tissue while avoiding information loss in pathological tissues, a window width of 80 HU and window center of 80 HU was used in this study.

After the contrast adjustment, a skull stripping method described in [8] was followed to extract brain tissues. For each CT slice, a rectangular contour was initialized around the center of the head. Then, the distance regularized level set evolution algorithm [9] was used to evolve the initialized contour to fit the border of the brain region enclosed by the skull. An example of contrast adjustment and skull stripping is shown in Fig. 2(a)–(b). The image after skull stripping is denoted as I_b .

2.2 Superpixel Generation

After pre-processing, we used the simple linear iterative clustering (SLIC) algorithm [10] to over-segment I_b into superpixels. The SLIC algorithm generates a group of coherent pixel collections based on color and spatial proximity (shown in Fig. 2(c)). There are many advantages of using superpixels. First, instead of processing every image pixel, using superpixels where similar pixels are clustered can reduce computation cost efficiently. Secondly, superpixels divide the entire image into meaningful image patches. Features extracted from superpixels can better characterize regional information. Considering that superpixels adhere to edges within an image (as exhibited in Fig. 2(c)), image segmentation can be performed via superpixel classification. In this work, we performed feature extraction on superpixels and classify those superpixels as belonging to hematoma regions or not. Based on these classification results, a coarse hematoma segmentation can be generated. In this study, I_b was over-segmented into approximately 5000 superpixels (each superpixel includes approximately 30 pixels).

2.3 Feature Extraction

A total of 63 features were extracted to describe the characteristics of superpixels.

Intensity Statistics. The mean, variance, skewness, and kurtosis of intensities in each superpixel were calculated. The mean value measures the average intensity level while the variance measures heterogeneity. The skewness and kurtosis describe the asymmetry and the tailedness, respectively. As different ranges of Hounsfield units correspond to different anatomical structures, these intensity statistics can help to describe superpixels.

Gabor Filters. A Gabor filter is a linear filter used for edge detection and textural analysis. The real component of a Gabor filter (assumed to be centered at zero) can be written as

$$g(x, y; \lambda, \theta, \psi, \sigma, \gamma) = \exp\left(-\frac{x'^2 + \gamma^2 y'^2}{2\sigma^2}\right) \cos\left(2\pi \frac{x'}{\lambda} + \psi\right),$$

$$x' = x \cos \theta + y \sin \theta,$$

$$y' = -x \sin \theta + y \cos \theta,$$
(3)

where (x,y) is the location of the Gabor filter. λ and ψ represent the wavelength and phase offset of the sinusoidal wave, respectively. θ and σ represent the orientation and standard deviation of the Gaussian envelope, respectively, while γ is the spatial aspect ratio.

In this study, we used a bank of Gabor filters introduced in [11]. 2-D Gabor filters oriented at 0, 30, 60, 90, 120, and 150° with wavelengths of $2\sqrt{2}$, $4\sqrt{2}$, $8\sqrt{2}$, and $16\sqrt{2}$ were used to calculate the response map at $\gamma=0.5$, $\psi=0$ and $\sigma=0.5$ λ . The mean and variance of Gabor responses at each superpixel were calculated as Gabor features as well as the dominant spatial frequency and its orientation.

Saliency. Saliency can be constructed as visual attention. In this study, a low-level approach was employed to determine the saliency of a superpixel by computing the average Euclidean distance of its mean intensity with 50 other superpixels that were randomly selected from the same image. Different from other extracted features, the saliency value contains global information at the slice level. From our observation, CT slices located close to the top of the head have a higher intensity value due to the partial volume effect. The saliency measurement can suppress the effect from this slice-level intensity shift. Also, it can help reduce the variability in intensity for the same tissue across different cases.

Gray-Level Co-Occurrence Matrix. A 16×16 patch around the center of each superpixel was taken to calculate the gray-level co-occurrence matrix (GLCM), which gives the joint probability distribution of gray-level pairs of

neighboring pixels. Let $\Omega_p = \{1, 2, \dots, N_{level}\} \times \{1, 2, \dots, N_{level}\}$, where N_{level} is the number of levels that gray intensities were quantized into. In this study, $N_{level} = 8$. Second-order statistics of the GLCM were used as features, specifically contrast, energy, and homogeneity, which are calculated as

$$contrast = \int_{\Omega_p} |i - j|^2 p(i, j) di \, dj, \tag{4}$$

$$energy = \int_{\Omega_p} p(i,j)^2 di \, dj, \tag{5}$$

$$homogeneity = \int_{\Omega_p} \frac{p(i,j)}{1 + |i-j|} di \ dj, \tag{6}$$

where p(i, j) is the value of GLCM at location (i, j).

Wavelet Packet Transformation. A two-level discrete Haar wavelet packet transformation [12] was applied to a 16×16 patch around the center of each superpixel. The image patch was decomposed into 8 bands, with each band containing information of different frequencies. The energy of coefficients in each band was computed and the percentages of energy corresponding to the details were used as regional features to characterize each superpixel.

2.4 Active Learning

Active learning is a method [13] to train a supervised classifier with the smallest annotated training dataset possible. As shown in Algorithm 1, the proposed active learning strategy started with training an initial SVM model using the initial training dataset, which consists of superpixels from only one labeled CT scan. After that, the initial model was used to classify superpixels from the pool dataset, which contains CT scans from 49 patients. Based on the predicted possibilities, we calculated the conditional Shannon entropy of each superpixel as

$$H_{\Theta}(s_i) = -\sum_{\hat{y} \in \{0,1\}} p_{\Theta}(y_i = \hat{y} | \boldsymbol{v}_i) \log(p_{\Theta}(y_i = \hat{y} | \boldsymbol{v}_i)), \tag{7}$$

where Θ denotes the trained SVM model. v_i and y_i are the feature vector and label of s_i , respectively. $p_{\Theta}(y_i = \hat{y}|v)$ denotes the predicted probability that s_i belongs to the corresponding class.

 $H_{\Theta}(s_i)$ is used as an uncertainty measurement for s_i . A high $H_{\Theta}(s_i)$ indicates that the trained model is uncertain about which class s_i belongs to. This may occur if s_i is under-represented in the current training dataset. Thus superpixels with high uncertainty values are the most informative samples to update the model. In our work, superpixels were ranked based on their uncertainty measurements in descending order and the top N_{al} superpixels were selected to be annotated and added into the training dataset. Next, an updated SVM

model was trained and the uncertainty measurements of the superpixels in the pool dataset were re-calculated. After the final SVM classifier was trained, coarse hematoma segmentation maps were generated by classifying superpixels in brain images.

Algorithm 1. Active Learning Strategy

Input: Labeled training dataset \mathcal{D}_l , unlabeled pool dataset \mathcal{D}_p , the number of iterations N_{iter} , the number of samples selected for query at each iteration N_{al}

Output: SVM classifier Θ^*

- 1: Train an initial SVM model Θ_0 on \mathcal{D}_t
- 2: for k = 1, k++, while $k <= N_{iter}$ do
- Use the trained SVM classifier Θ_{k-1} to measure the uncertainty of superpixels
- Select N_{al} most informative samples $\{v_1^{(k)}, v_2^{(k)}, ..., v_{N_{al}}^{(k)}\}$ from \mathcal{D}_p . 4:
- 5:
- Update \mathcal{D}_p : $\mathcal{D}_p = \mathcal{D}_p \{\boldsymbol{v}_1^{(k)}, \, \boldsymbol{v}_2^{(k)}, \, ..., \, \boldsymbol{v}_{N_{al}}^{(k)} \}$ Query the physician for labels $\{l_1^{(k)}, l_2^{(k)}, ..., l_{N_{al}}^{(k)} \}$ of the selected samples 6:
- Update \mathcal{D}_t : $\mathcal{D}_t = \mathcal{D}_t \bigcup \{ (\boldsymbol{v}_1^{(k)}, l_1^{(k)}), (\boldsymbol{v}_2^{(k)}, l_2^{(k)}), ..., (\boldsymbol{v}_{N_{s,l}}^{(k)}, l_{N_{s,l}}^{(k)}) \}$ 7:
- Train an SVM model Θ_k on the updated \mathcal{D}_t .
- 9: end for
- 10: Return $\Theta^* = \Theta_{N_{iter}}$

2.5 **Active Contour Model**

A region-based active contour model [14] was extended by incorporating coarse hematoma segmentation to improve the segmentation performance. In an active contour model, a dynamic contour evolves iteratively by minimizing the energy function. In this work, the energy function is defined as a combination of a region-based term, a prior shape term, and a regularization term. The shape term was added to give a penalty when the evolving contour at the t^{th} iteration deviates from the prior shape.

Let $\phi: \Omega \to \mathbb{R}$, $\Omega = \{1, 2, \dots, H\} \times \{1, 2, \dots, W\}$ be the level function of an Euclidean signed distance function. The contour is represented by $\mathcal{C} = \{x \in \mathcal{C} \mid x \in \mathcal{C} \}$ $\Omega|\phi(x)=0\}$, where points inside the contour have $\phi(x)>0$ and points outside the contour have $\phi(x) < 0$. Given an image I_b , let \mathcal{C}_{SVM} denote the predicted hematoma contour from the SVM classifier, with ϕ_{SVM} the corresponding level set function. ϕ_{SVM} is used both as an initial contour $\phi^{(0)}$ for curve evolution and a prior shape for shape constraints. The energy function can be written as

$$E(\phi) = E_{region}(\phi) + \alpha_1 E_{shape}(\phi) + \alpha_2 E_{reg}(\phi), \tag{8}$$

$$E_{region}(\phi) = \int_{\Omega} |I_b(\boldsymbol{x}) - c_1|^2 H(\phi(\boldsymbol{x})) d\boldsymbol{x} + \int_{\Omega} |I_b(\boldsymbol{x}) - c_2|^2 (1 - H(\phi(\boldsymbol{x}))) d\boldsymbol{x},$$
(9)

$$E_{shape}(\phi) = \int_{\Omega} (\phi(\boldsymbol{x}) - \phi_{SVM}(\boldsymbol{x}))^2 d\boldsymbol{x}, \tag{10}$$

where $H(\cdot)$ is the Heaviside function. $\nabla(\cdot)$ is the gradient operation. E_{reg} follows the formula proposed in [9], whose role is to maintain the signed distance property $|\nabla \phi(\mathbf{x})| = 1$ within the vicinity of the zero level set. c_1 and c_2 in (9) are the average of I_b inside and outside \mathcal{C} , respectively. They are calculated as

$$c_1(\phi) = \frac{\int_{\Omega} I_b(\mathbf{x}) H(\phi(\mathbf{x})) d\mathbf{x}}{\int_{\Omega} H(\phi(\mathbf{x})) d\mathbf{x}}$$
(11)

and

$$c_2(\phi) = \frac{\int_{\Omega} I_b(\boldsymbol{x})(1 - H(\phi(\boldsymbol{x})))d\boldsymbol{x}}{\int_{\Omega} (1 - H(\phi(\boldsymbol{x})))d\boldsymbol{x}}.$$
 (12)

The final contour can be obtained by using the gradient descent algorithm to minimize the energy function over ϕ :

$$\phi^* = \operatorname*{argmin}_{\phi} E(\phi). \tag{13}$$

The active contour model proposed in this study was used to smooth the boundary of coarse hematoma segmentation.

2.6 Evaluation Metrics

To evaluate the performance of a trained SVM model on superpixel-based classification, the precision, recall, and accuracy were calculated, as well as the Dice coefficient between the coarse segmentation and manual segmentation. After the active contour algorithm, the final fine segmentation was evaluated by calculating pixel-based precision, recall, accuracy, and Dice coefficient between the final segmentation and manual segmentation. All measures were patient-wise and averaged over patients in the test set.

3 Experimental Results and Discussion

3.1 Dataset

Our dataset consists of 35 head CT scans from the Progesterone for Traumatic brain injury: Experimental Clinical Treatment (ProTECT) study [15] and 27 brain CT scans from University of Michigan Health System. The brain scans are from patients who experienced a moderate to severe head injury and were enrolled in an emergency department within 4 h of their injury. In total, 2433 axial CT images from 62 patients who suffered from acute TBI were used in this study, with image slice thickness ranging from 3.0 to 5.0 mm. To validation our proposed hematoma segmentation framework and active learning strategy, 13 cases were annotated as the test set by an experienced medical expert, who examined 2D cross-sectional slices and then manually drew the boundary around hematoma regions. We used the remaining 49 cases as the training set, wherein each experiment of active learning one slice was randomly selected and annotated as the initial training set while all others were used as the pool set.

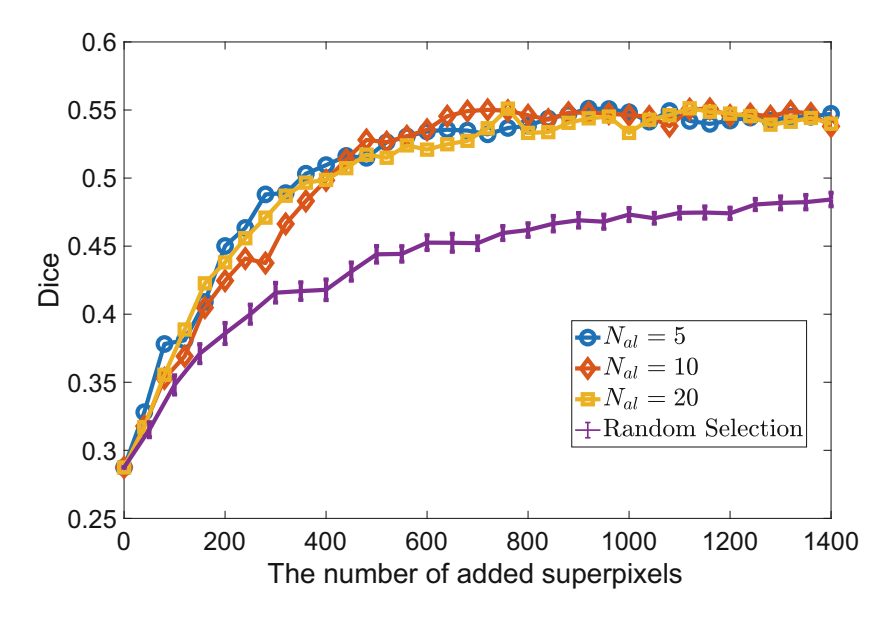


Fig. 3. Comparison of active learning with $N_{al} = 5, 10, 20$ and random selection. The Dice coefficients of random selection with different numbers of added superpixels are averaged over 50 experiments. 95% confidence intervals are also given.

3.2 Active Learning

An initial SVM model was trained on the initial training set using a linear kernel. We then used the active learning strategy to select the most informative superpixels, which were then annotated, gradually improving the performance of the model. Several experiments were performed to explore the performance of classifiers with the same initial training set while varying N_{al} . From Fig. 3, the curves tend to plateau after 1000 newly labeled superpixels are added with active learning, and the effect of N_{al} on the final performance is not significant. In contrast to active learning strategy, an SVM classifier was trained as a baseline on the initial training set and a fixed number of randomly selected superpixels from the pool set (shown as 'Random Selection' in Fig. 3). 50 independent experiments were performed and the results were averaged to represent the performance of using random selection. From Fig. 3, with the same number of added superpixels, the performance of the SVM model trained using the active learning strategy is significantly higher than the baseline. After adding over 1000 additional samples, the model trained with active learning achieved an average Dice coefficient of 0.55 over 13 patients.

To further examine the robustness of active learning algorithm over different initial datasets, we repeated the above active learning algorithm and random selection method for 20 times, respectively. For each time, one slice was randomly selected and annotated as the initial training set while other slices in the training set were used as the pool set. Each SVM classifier using active learning were trained

Table 1. Comparison of the active learning strategy and random selection method using 20 different initial training sets. n is the number of additional superpixels added to the initial training set. The mean and standard derivation (stddev) of evaluation measurements over 20 experiments are given in the format of mean (stddev).

	Dice	Precision	Recall	Accuracy
Active Learning $(n = 1000)$	0.55 (0.01)	0.59 (0.02)	0.60 (0.02)	0.97 (0.01)
Random Selection $(n = 1000)$	0.47 (0.02)	0.45 (0.02)	0.61 (0.03)	0.94 (0.01)
Random Selection $(n = 5000)$	0.54 (0.01)	0.57 (0.02)	0.60 (0.02)	0.96 (0.01)

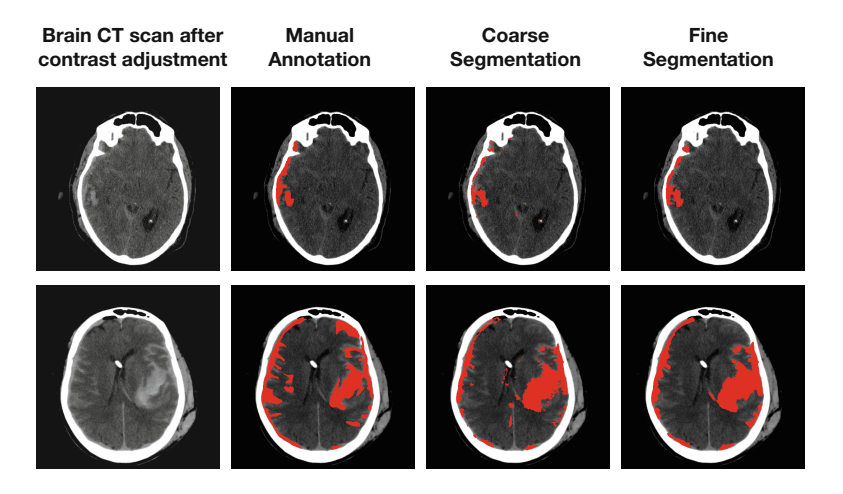


Fig. 4. Segmentation results. Each row gives an example of the segmentation compared with the manual segmentation. The segmented or annotated hematoma regions are shown in red (Color figure online).

on the initial training set and 1000 additional samples selected with $N_{al} = 5$. The comparison of performance metrics between active learning and random selection is shown in Table 1. Our final SVM models from active learning have comparable performance with random selection models trained on the same initial training sets added with five times more annotated superpixels. The standard derivations of measures over experiments are very small.

3.3 Segmentation

After constructing the coarse hematoma segmentation for each slice via a trained SVM classifier, the proposed active contour model was performed to refine the boundary. An additional 10 CT slices in the pool set were annotated to tune the parameters for active contour. Finally, we used $\alpha_1 = 2, \alpha_2 = 0.5, \epsilon = 0.05$ and the step size $\mu = 0.2$. From Fig. 4, the coarse segmentation has an accurate hematoma localization while the boundary is rough, which may be due to

Table 2. Segmentation performance comparison. The patient-wise mean and standard derivation (stddev) of evaluation measurements are given in the format of mean (stddev).

	Dice	Precision	Recall	Accuracy
Coarse segmentation	0.55 (0.21)	0.62 (0.23)	0.59 (0.18)	0.97 (0.03)
Fine segmentation	0.60 (0.19)	0.63 (0.23)	0.67 (0.16)	0.98 (0.03)
GMM [7]	0.46 (0.22)	0.45 (0.23)	0.60 (0.18)	0.94 (0.06)

superpixel sampling. The active contour model can help smooth the boundary and improve segmentation accuracy. From Table 2, the proposed active contour model greatly improved the segmentation performance. Additionally, our method significantly outperformed a previous method named GMM [7].

4 Conclusion

Automatic and accurate hematoma segmentation is important for TBI patient management. In this study, a combination of active learning and an active contour model was proposed for hematoma segmentation in acute cases. In supervised SVM training, statistical and textural features were extracted to characterize superpixels over-segmented from brain images. With the proposed active learning strategy, an SVM classifier was trained on a very small amount of annotated data. After that, the coarse segmentation from the SVM classifier was incorporated into the active contour model to generate fine hematoma segmentation. The overall segmentation method achieved a mean dice of 0.60 in a highly heterogeneous dataset. Our experiments show that an active learning strategy can effectively select the most informative data points from a highly imbalanced and varied data pool. From our results, active learning is potential to overcome the shortage of annotated data in medicine.

For future work, we will continue working on the active learning strategy. In our current framework, during the active learning, the selected superpixels will be highlighted in the brain images and presented to clinicians for annotation. Considering annotating 1000 superpixels is still not an easy task, further informativeness measurements will be designed to find the most informative image patches or CT slices to reduce the labor required in the annotation phase of active learning.

Acknowledgment. The work is supported by National Science Foundation under Grant No. 1500124.

References

 Lee, B., Newberg, A.: Neuroimaging in traumatic brain imaging. NeuroRx 2(2), 372–383 (2005)

- Broderick, J.P., Brott, T.G., Duldner, J.E., Tomsick, T., Huster, G.: Volume of intracerebral hemorrhage. a powerful and easy-to-use predictor of 30-day mortality. Stroke 24(7), 987–993 (1993)
- 3. Jacobs, B., Beems, T., van der Vliet, T.M., Diaz-Arrastia, R.R., Borm, G.F., Vos, P.E.: Computed tomography and outcome in moderate and severe traumatic brain injury: hematoma volume and midline shift revisited. J. neurotrauma 28(2), 203–215 (2011)
- Chesnut, R., Ghajar, J., Gordon, D.: Surgical management of acute epidural hematomas. Neurosurgery 58(3), S2-7 (2006)
- Bardera, A., et al.: Semi-automated method for brain hematoma and edema quantification using computed tomography. Comput. Med. Imaging Graph. 33(4), 304–311 (2009)
- Liao, C.C., Xiao, F., Wong, J.M., Chiang, I.J.: Computer-aided diagnosis of intracranial hematoma with brain deformation on computed tomography. Comput. Med. Imaging Graph. 34(7), 563–571 (2010)
- Soroushmehr, S.M.R., Bafna, A., Schlosser, S., Ward, K., Derksen, H., Najarian, K.: CT image segmentation in traumatic brain injury. In: 37th Annual International Conference of the IEEE Engineering in Medicine and Biology Society (EMBC), pp. 2973–2976. IEEE (2015)
- 8. Farzaneh, N., et al.: Automated subdural hematoma segmentation for traumatic brain injured (TBI) patients. In: 39th Annual International Conference of the IEEE Engineering in Medicine and Biology Society (EMBC), pp. 3069–3072. IEEE (2017)
- Li, C., Xu, C., Gui, C., Fox, M.D.: Distance regularized level set evolution and its application to image segmentation. IEEE Trans. Image Process. 19(12), 3243–3254 (2010)
- Achanta, R., Shaji, A., Smith, K., Lucchi, A., Fua, P., Süsstrunk, S., et al.: Slic superpixels compared to state-of-the-art superpixel methods. IEEE Trans. Pattern Anal. Mach. Intell. 34(11), 2274–2282 (2012)
- 11. Jain, A.K., Farrokhnia, F.: Unsupervised texture segmentation using gabor filters. Pattern Recognit. **24**(12), 1167–1186 (1991)
- Rioul, O., Vetterli, M.: Wavelets and signal processing. IEEE Signal Process. Mag. 8(4), 14–38 (1991)
- 13. Settles, B.: Active learning. Synth. Lect. Artif. Intell. Mach. Learn. **6**(1), 1–114 (2012)
- Chan, T.F., Vese, L.A.: Active contours without edges. IEEE Trans. Image Process. 10(2), 266–277 (2001)
- 15. Wright, D.W., et al.: Protect: a randomized clinical trial of progesterone for acute traumatic brain injury. Ann. Emerg. Med. **49**(4), 391–402 (2007)